Defect states of chemical vapor deposition grown GaN nanowires: Effects and mechanisms in the relaxation of carriers

Demetra Tsokkou,[1] Andreas Othonos,[1,a)] and Matthew Zervos[2]
[1]*Department of Physics, Research Center of Ultrafast Science, University of Cyprus, P.O. Box 20537, 1678 Nicosia, Cyprus*
[2]*Department of Mechanical and Manufacturing Engineering, Nanostructured Materials and Devices Laboratory, Materials Science Group, University of Cyprus, P.O. Box 20537, 1678 Nicosia, Cyprus*

(Received 4 June 2009; accepted 31 July 2009; published online 9 September 2009)

Carrier relaxation in GaN nanowires, grown by atmospheric pressure chemical vapor deposition, via direct nitridation of Ga with NH_3 at 950 °C has been investigated in detail. Differential absorption measurements reveal a large number of defect states located within the band gap. The relaxation dynamics of the photogenerated carriers suggest three distinct regions of energy states below the band edge identified as *shallow donor states*, *midgap states*, and *deep acceptor states*. Measurements suggest that Auger recombination is not a contributing factor in carrier relaxation even at the highest fluence (~ 1 mJ/cm^2) used in this work for carriers located within the conduction band. On the contrary, Auger recombination has been observed when probing the shallow donor states for fluences above 40 μJ/cm^2. Measurements at the lowest fluence reveal a biexponential relaxation for the donor states with the fast component (~ 50 ps) corresponding to the relaxation of carriers into the midgap states and the slow component of 0.65 ns associated with the relaxation into the deep acceptor states. Measurements reveal free-carrier absorption contribution from the deep acceptor states to the *U*-valley with an observed threshold limit of 3.5 eV suggesting the *U*-valley is located approximately 4.7 eV from the valence band. © *2009 American Institute of Physics*. [doi:10.1063/1.3212989]

I. INTRODUCTION

Group III-nitride (III-N) compound semiconductors, and especially GaN, InN, AlN, and their ternary or quaternary alloys, have proven to be useful for electronic and optoelectronic devices and have been investigated extensively over the past decade.[1–5] GaN epitaxial layers are an interesting material for optoelectronic devices emitting in the blue and ultraviolet (UV) regions and have already been utilized not only in commercial light emitting diodes and lasers[6–8] but also for the fabrication of UV photodetectors[9] due to the direct band gap, which is equal to 3.4 eV at room temperature (RT). Additionally, GaN has been used in high temperature, power electronic devices[10] such as field effect transistors.[11,12] On the other hand, III-N nanostructures, and especially nanowires (NWs), are interesting, since the lattice mismatch between GaN and the substrate on which they are grown is not so much of a severe constraint as in the case of homo- or heteroepitaxial growth of GaN. As a consequence, improved control on the formation of defects is feasible, which will potentially lead to nanodevices with enhanced performance and the possibility of direct integration with mainstream Si devices. In view of this, a great deal of work has been done in determining the growth conditions and investigating the structural, optical, and electrical properties of GaN NWs.[13] GaN NWs have already been grown not only by different methods, such as chemical vapor deposition (CVD),[13] metal organic CVD,[14] and molecular beam epitaxy,[15] but also via the arc discharge method,[16] pyrolysis,[17] and pulsed laser ablation.[18]

Given the potential impact that GaN may have in optoelectronic applications, it is of great importance to understand not only the fundamental behavior of photogenerated carriers upon excitation and their subsequent relaxation, but also the dominant relaxation mechanisms in this nanostructured material. Previous studies on the optical properties of GaN NWs have focused on steady-state photoluminescence (PL) measurements.[13,19,20] While the dynamic carrier behavior has been extensively investigated for bulk GaN,[21–23] carrier dynamics in GaN NWs and, in particular, the role of defect-related states within the band gap on carrier relaxation have not been investigated. Specifically only time resolved PL measurements have been reported.[24,25] In this work, transient absorption measurements were performed in GaN NWs using a nondegenerate pump-probe technique with above and below band gap excitation. Femtosecond laser pulse excitation provides the required temporal resolution for investigating carrier dynamics on an ultrafast time scale and so time resolved absorption spectroscopy provides an important insight into relaxation of the photogenerated carriers into energy states located above and below the conduction band (CB) edge.

II. EXPERIMENTAL PROCEDURE

GaN NWs were grown, initially, on *n* type Si (111) and then on sapphire (Al_2O_3) via atmospheric pressure CVD and direct nitridation of metal Ga with NH_3. Initially a thin film

a)Electronic mail: othonos@ucy.ac.cy.

of Au with thickness of ≈0.5 nm was deposited on Si(111) or Al_2O_3 via sputtering at a slow rate <5 Å/s using an Ar ion plasma. Before the deposition of Au film, substrates were cleaned in HF, rinsed in ionized water, and dried with nitrogen. The Au-coated substrate was placed in an alumina boat and then ≈0.3 g of pure metal Ga (Aldrich 99.99%) was carefully placed in the boat <5 mm upstream from the sample. The boat was then loaded at the center of a 25 mm quartz tube directly above the thermocouple used to measure the heater temperature. Initially, the tube was flushed with 500 SCCM (SCCM denotes cubic centimeter per minute at STP) of Ar and 500 SCCM of N_2 containing 5% H_2, for 10 min in order to eliminate residual oxygen and moisture contained in the reactor. Afterwards, the temperature of the furnace was increased to 950 °C with a ramp rate of 15 °C/min, under a steady flow of 100 SCCM of N_2:5%H_2. Subsequently, the temperature was maintained at 950 °C for 1 h and NH_3 was allowed to flow at 25 SCCM using a reduced flow of 75 SCCM of N_2:5%H_2. At the end of the growth period the reactor was allowed to cool down to RT in flows of 25 SCCM of NH_3 and 75 SCCM of N_2:5%H_2. Upon removal from the reactor the Si or Al_2O_3 substrates were covered with a white-blue colored layer. The morphology of the GaN NWs was investigated by using a TESCAN scanning electron microscope (SEM), and the crystal structure and phase purity of the NWs were determined by x-ray diffraction (XRD) using a SHIMADZU XRD-6000 diffractometer and Al holders.

Transient absorption measurements were performed using two different ultrafast amplifier laser systems in a typical supercontinuum pump-probe configuration.[26] The first system contains a self mode-locked Ti:sapphire generating 35 fs, 5 nJ pulses at ~800 nm with a repetition rate of 100 MHz. A regenerative amplifier is used to intensify the pulses approximately 10^6 times at a repetition rate of 5 kHz. An optical parametric amplifier was utilized to generate excitation pulses in the UV region of the spectrum for above band gap excitation of the GaN NWs. A small part of the fundamental energy was used to generate a supercontinuum white light in the visible/near infrared region of the spectrum for transient nondegenerate absorption measurements. Additionally, a second harmonic crystal was used in a different setup to double the frequency of the fundamental light for the generation of white light continuum in the UV region. Moreover, a second ultrafast amplifier system uses a similar apparatus to produce excitation pulses at 400 nm with time duration of 100 fs and a repetition rate of 1 kHz.

III. RESULTS AND DISCUSSION

So far GaN NWs have been grown by the direct nitridation of metal Ga with NH_3,[13,27–29] at temperatures above 900 °C due to the reduced vapor pressure of Ga at lower temperatures. In order to enhance the vapor pressure of Ga at lower growth temperatures Chang and Wu[30] used Ga acetylacetonate as a precursor, and, more recently, Yu *et al.*[31] used a mixture of Ga and CaF_2.[31] Different metals have been used as a catalyst for the synthesis of GaN NWs, such as transitions metals Ni,[27,28,31] Fe,[13] In,[13] and Co.[13] However, controversial results have been reported when Au is used as a catalyst, since Cai *et al.*[27] reported the synthesis of GaN NWs with this catalyst, while Zhang and Zhang[28] mentioned that no wires were formed. A typical SEM image of the high density GaN NWs grown on 0.5 nm Au/Al_2O_3 is shown in Fig. 1. Straight wires with uniform diameters of ≈100 nm and lengths up to a few microns are observed. Figure 2 shows the XRD pattern of the GaN NWs grown on sapphire where the peaks correspond to the (100), (002), (101), (110), and (112) crystallographic planes of the hexagonal wurtzite structure of GaN with lattice constants a=0.318 nm and c=0.518 nm.[29] In agreement with previous investigations on GaN NWs,[13,27–29] high growth temperatures ≥900 °C are necessary for the growth of GaN NWs by direct nitridation of metal Ga with NH_3. NWs were also obtained at 900 °C, but their density was higher at 950 °C. We also found that the addition of H_2 to the gas flow, during the temperature ramp and growth step, is crucial to prevent the oxidation of

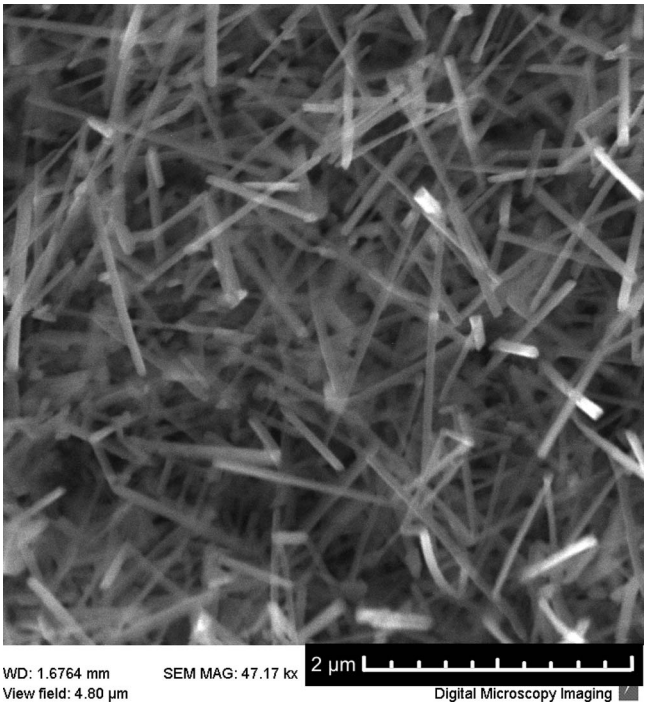

FIG. 1. SEM image of the GaN NWs on Au/Al_2O_3.

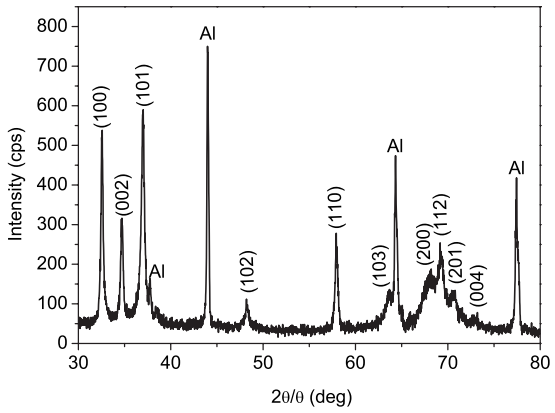

FIG. 2. XRD pattern of GaN NWs on sapphire.

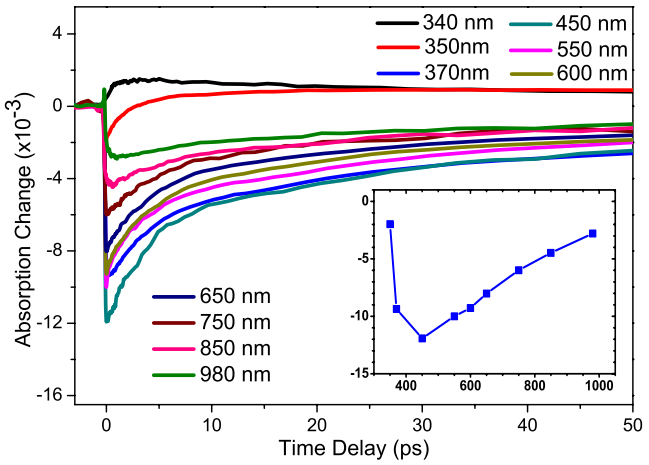

FIG. 3. (Color online) Nondegenerate, time resolved, transient absorption measurements of the GaN NWs using ultrafast excitation pulses at 320 nm and probing pulses in the range 340–980 nm. In the inset state filling minimum is shown vs probing wavelength.

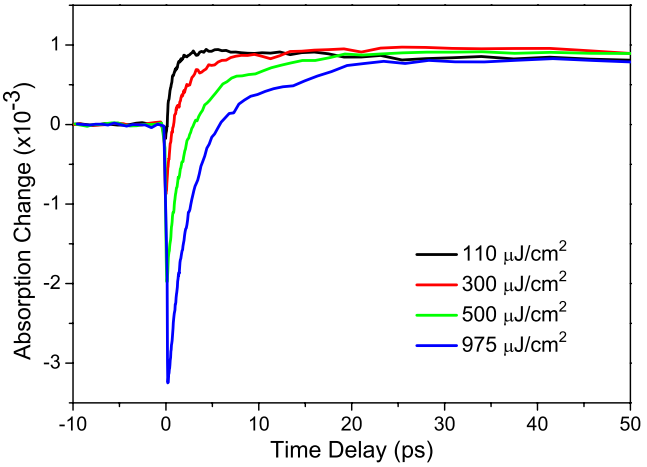

FIG. 4. (Color online) Nondegenerate, time resolved, transient absorption measurements of the GaN NWs using ultrafast excitation pulses at 320 nm and probing pulses at 350 nm for different pump fluences.

Ga from residual O_2 in the reactor. In addition when NH_3 was included during the temperature ramp it leads to the nitridation of the Ga upstream, which in turn reduced the vapor pressure at the growth temperature. No GaN NWs were obtained on silicon or sapphire alone confirming that the GaN NWs grow by the vapor-liquid-solid mechanism. In contrast with a previous study[28] Au is a proper choice for the growth of GaN NWs.

Figure 3 shows transient absorption nondegenerate measurements using UV femtosecond pulse excitation and, in particular, the time evolution of absorption change for excitation pulses at 320 nm (3.87 eV) and different probing wavelengths ranging between the UV and near IR region of the spectrum. Measurements were carried out for delays up to 500 ps, although only 50 ps are shown in Fig. 3 for clarification purposes. The absorbed pump fluence for these data was estimated to be $\sim 0.5\ \mathrm{mJ/cm^2}$. Also seen as an inset in Fig. 3 is the state filling minimum signal, which is plotted as a function of probing wavelength. Clearly evident from the data in Fig. 3 is the different temporal behavior of the induced absorption for probing wavelengths corresponding to photon energy above and below the band edge of the GaN NWs. What appears to be common in all the curves is a fast initial response reaching a minimum or maximum depending on the probing wavelength, which is then followed by a slower recovery toward equilibrium. It is well known that above band gap excitation of a semiconductor material will result in the generation of carriers that will occupy the available energy states near the excitation region. As a consequence of this occupation of states, a negative change in absorption is expected, known as state filling. However, in addition to state filling, free carriers may undergo secondary excitation by the probe laser pulse resulting in what is known as "free-carrier absorption." This is a positive contribution to the induced absorption and it usually competes with state filling, which is negative. Normally state filling is the dominant contribution when probing above the band edge, whereas free-carrier absorption is the dominant process when probing below the band edge. It is interesting to point out that in the CVD grown GaN NWs when probing at 340 nm, which is above the band edge, we notice a positive signal suggesting that free-carrier absorption is the dominant contribution. Although this is not expected, we believe that as a consequence of strong coupling between the photogenerated carriers and energetically higher states with an energy difference corresponding to the probing wavelength, free-carrier absorption prevails.

A more complex behavior is observed when probing at 350 nm. State filling is initially observed, but with increasing delay time the signal becomes positive before it returns to equilibrium. Furthermore, strong state filling effects are observed for all probing wavelengths between 370 and 980 nm. This result suggests that defect-related states are located within the entire band gap of the GaN NWs. This is clearly seen in the inset of Fig. 3 where state filling minimum versus wavelength is shown and which to a first approximation reflects the density of states at the probing wavelength.

To further investigate the transient behavior of the GaN NWs, intensity measurements have been carried out at the probing wavelength of 350 nm, as seen in Fig. 4. Clearly evident is the initial negative state filling, which is intensity dependent. This observed state filling is associated with the occupation of states located near the band edge, so we need to consider the possibility that the observed positive signal in the temporal profiles of the measurements could be due to band gap renormalization, as has already been reported in degenerated pump-probe measurements for bulk GaN.[32] Nevertheless, in nondegenerate transient absorption measurements, band gap renormalization would be expected to be observed first, followed by state filling when the carriers reach the probing state. Furthermore, the maximum positive signal and its temporal behavior do not exhibit any dependence on the incident fluence and thus on the photogenerated carrier density. In view of the above, it is believed that the positive signal in Fig. 4 is not associated with band gap renormalization, but rather with free-carrier absorption.

In what follows we will explain in more detail the observed free-carrier absorption at 350 nm. It is important to point out that the different temporal behavior observed for

state filling and free-carrier absorption suggests that these contributions are related to different energy states. The state filling signal appears to increase linearly with increasing pump fluence. This observation is consistent with the fact that higher pump fluences lead to larger occupation of states in the CB by the photogenerated carriers. It is worthy to mention that with increasing pump fluence, state filling appears to take longer, suggesting that Auger recombination is negligible for states in the CB located around 3.5 eV, even for the highest fluences (~ 1 mJ/cm^2) used in this work. For longer delay times free-carrier absorption appears to dominate. Furthermore, the relaxation of this signal appears to be almost identical for all pump fluences as seen in the inset of Fig. 4. This suggests that the two competitive effects are not influenced in the same way by the increment in pump energy, despite that both effects are carrier density dependent. The observations above suggest that the saturation of free-carrier absorption occurs even for the lowest pump energy used in these experiments. We should also note that in the measurements of Fig. 3, no free-carrier absorption is observed for probing wavelengths larger than 350 nm (3.5 eV), setting a minimum limit for the energy difference between the coupled states where free-carrier transitions take place. Given the above observations, it is believed that free-carrier transitions take place between a defect-related state located inside the band gap and the indirect satellite valley of the CB. The possibility that free-carrier transitions may occur between states in the CB is ruled out given the intensity dependent measurements of Fig. 4. In interpreting our experimental results we took into consideration a theoretical model for the distribution of defect states in GaN proposed by Shalish *et al.*[33] According to this model, deep acceptor states correlated with the yellow luminescence are attributed to Ga vacancies, which are centered at ~ 1.2 eV from the top of the valence band. Taking into consideration the minimum energy difference between the energy states for the observation of free-carrier absorption (~ 3.54 eV), we conclude that the energy difference between the indirect valley and valence band is ~ 4.7 eV. This result is in very good agreement with the minimum energy of the *U*-valley (~ 4.73 eV) for the bulk wurtzite GaN reported by Sun *et al.*[21] No changes in the energy states are expected due to quantum confinement effects, since the diameter of the wires is much larger than the exciton Bohr radius for this material.[34]

To help the reader obtain a clear picture of the dynamics in GaN NWs we have included a schematic band diagram model (Fig. 5) showing the various defect states and relaxation mechanisms utilized in our interpretation. The main relaxation mechanisms within the band gap are identified as "A–D." The transitions discussed above, between deep acceptor states (~ 1.2 eV) and states within the *U*-valley (~ 4.7 eV), and observed when the probing energy is larger than 3.5 eV are also shown with an arrow.

To further improve our understanding of the carrier dynamics in the GaN NWs intensity measurements have also been carried out at 370 nm thus probing energy states placed just below the direct band edge. The intensity measurements are normalized for comparison purposes and are shown in Fig. 6. The observed state filling is attributed to the occupation of shallow donor energy states due to nitrogen vacancies and oxygen impurities[35] by the photogenerated carriers. Clearly evident from the normalized data is that carrier relaxation becomes faster with increasing pump fluence indicating that Auger recombination is present. Given that Auger recombination was negligible for the carriers within the CB energy states (Fig. 4), we conclude that the observed Auger effects must arise from interactions of carriers within the defect-related states. Relaxation times for the lowest pump energy of 11 μJ/cm^2, where Auger recombination is expected to be negligible, have been estimated using multiple exponential decays. Best fitting was obtained using a biexponential decay corresponding to two relaxation mechanisms. The first mechanism with a time constant ≈ 50 ps

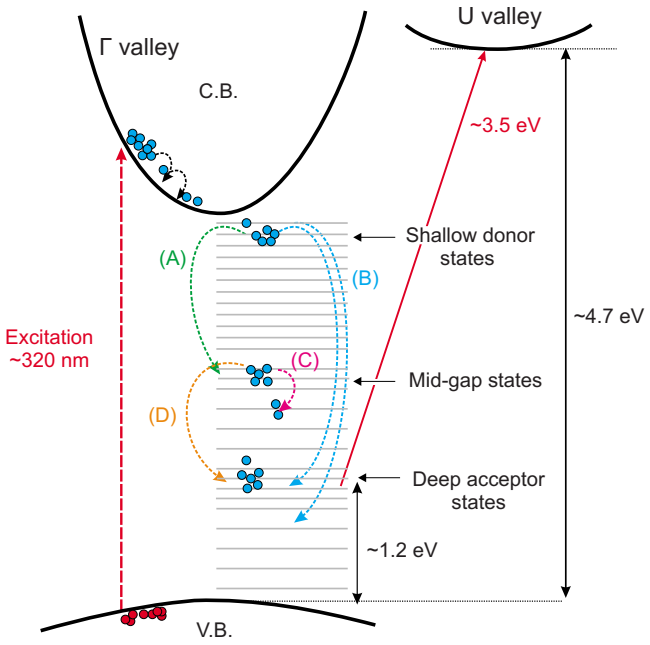

FIG. 5. (Color online) Schematic energy band diagram of GaN NWs. The excitation at 320 nm generating carriers within the CB is depicted as a vertical dashed arrow. Relaxation mechanisms within the band gap are identified as A–D (dot arrows). Free-carrier absorption from the deep acceptor states to the *U*-valley ($\Delta E \sim 3.5$ eV) is also shown in the diagram.

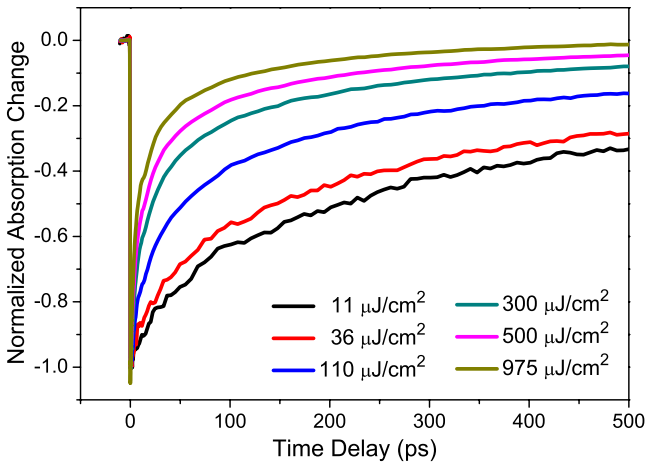

FIG. 6. (Color online) Normalized transient absorption change in the GaN NWs using ultrafast excitation pulses at 320 nm and a probing wavelength at 370 nm for different pump fluences.

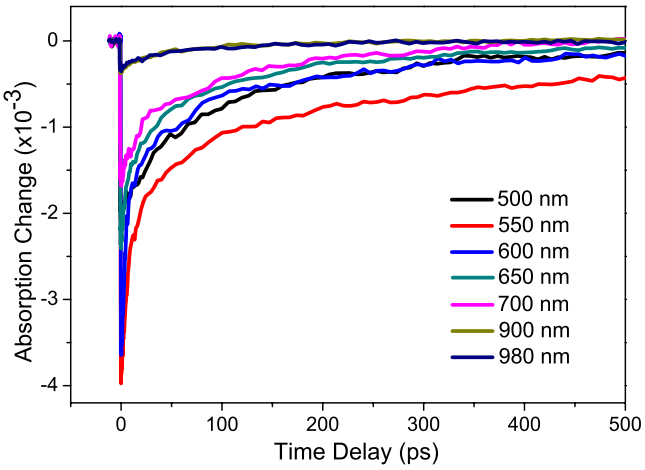

FIG. 7. (Color online) Nondegenerate transient absorption measurements of the GaN NWs using ultrafast excitation pulses at 400 nm and probing pulses in the range 340–980 nm.

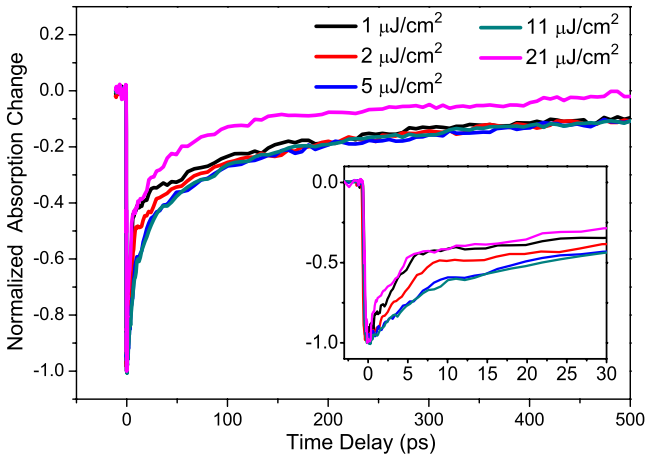

FIG. 8. (Color online) Nondegenerate transient absorption measurements of the GaN NWs using ultrafast excitation pulses at 400 nm and probing pulses at 550 nm for different pump fluences.

(30%) is attributed to carriers originating from native defects, or due to the surface of the NWs and relaxing to the midgap states. This mechanism is identified as mechanism A in Fig. 5. The second mechanism with a time constant of ≈655 ps (70%) is believed to be associated with carriers relaxing to the deep acceptor states inside the band gap i.e., mechanism B. Here we should point out that the latter mechanism may be responsible for the observed yellow luminescence (~2.30 eV) in GaN.[36] However, we cannot rule out the possibility that carriers may relax to lower shallow acceptor states or recombine.

To further investigate carrier dynamics within the defect-related states that are energetically located inside the band gap, nondegenerate time resolved absorption measurements have been performed using excitation at 400 nm (3.1 eV). The temporal measurements are shown in Fig. 7. The estimated absorbed pump fluence in these measurements is ~10 $\mu J/cm^2$. The induced absorption change when probing below the band edge reveals a large density of defect states. Here we should also point out that no signal was detected when the excitation wavelength was set to 650 nm (≡1.9 eV), even for pump energies ten times higher than the energy used at 400 nm, confirming that a much lower density of states exists in this region. Clearly evident from Fig. 7 is the dominant state filling, which prevails over free-carrier absorption for all probing wavelengths in the region between 500 and 980 nm. This behavior is in agreement with the previous results obtained for above band gap excitation. A comparison of the dynamics above and below band gap excitation reveals similar time constants when the absorption fluence was kept approximately constant.

Finally, intensity measurements were performed for excitation pulses at 400 nm, probing wavelength at 550 nm and for absorption fluences ranging between 1 and 21 $\mu J/cm^2$. Figure 8 shows the normalized intensity measurements for comparison purposes. The fast relaxation component as seen in the inset of Fig. 8 becomes slightly slower, i.e., increased from 6.5 to 12 ps (60%), as the fluence increased from 1 to 11 $\mu J/cm^2$. This is due to the larger number of carriers that occupy the defect-related states, and as a result these carriers need longer times to leave the probing region. It is believed that the fast relaxation time is associated with mechanism C in Fig. 5, which is the required time for probed carriers to relax to energetically close states. The slow relaxation component is estimated to be ~350 ps (40%) and is probably associated with nonradiative transitions to the lower acceptor states, which is identified as mechanism D in Fig. 5. For fluence higher than 11 $\mu J/cm^2$, a change in the temporal behavior of the induced absorption is observed. It appears that carrier relaxation becomes faster at 22 $\mu J/cm^2$, indicating that Auger recombination is present for the midgap states when a threshold in carrier density is exceeded.

IV. CONCLUSIONS

The effects on carrier relaxation of defect-related states inherit in CVD grown GaN NWs have been studied in detail. Transient absorption measurements reveal a large number of defect states located below the band edge. These states are placed throughout the entire band gap, and their presences were confirmed via state filling effects observed for all probing wavelengths below the band edge. A simplified band gap model, which incorporates three distinct regions of states, namely, shallow donor, midgap, and deep acceptor states located below the band edge, has been utilized to explain the carrier dynamics following femtosecond pulse excitation. Furthermore, it appears that Auger recombination is not a contributing factor in the carrier relaxation of carriers located within the CB even for the highest fluence used in this work. On the contrary, Auger recombination has been observed when probing the shallow donor states just below the band edge for fluences as low as 36 $\mu J/cm^2$. Measurements at the lowest fluence reveal a biexponential relaxation related to the donor states with the fast component corresponding to the relaxation carriers into the midgap states and the slow component of 0.65 ns associated with the relaxation into the deep acceptor states. Differential absorption measurements when probing above the band gap reveal free-carrier absorption contribution corresponding to coupling between the deep acceptor states located at 1.2 eV from the valence band and the indirect *U*-valley. The observed threshold limit of 3.5 eV to

the coupling between these states suggests that the *U*-valley is located approximately 4.7 eV from the valence band in the GaN NWs.

ACKNOWLEDGMENTS

The work in this article was supported by the Research Promotion Foundation of Cyprus under Grants EPYNE/0506/02, EPYAN/0506/04, BE0308/03 for fundamental research in the area of nanotechnology and nanomaterials.

[1]S. C. Jain, M. Willander, J. Narayan, and R. Van Overstraeten, Appl. Phys. Lett. **87**, 965 (2000).
[2]H. Hirayama, J. Appl. Phys. **97**, 091101 (2005).
[3]O. Ambacher, J. Phys. D **31**, 2653 (1998).
[4]A. G. Bhuiyan, A. Hashimoto, and A. Yamamoto, J. Appl. Phys. **94**, 2779 (2003).
[5]B. Monemar, J. Mater. Sci.: Mater. Electron. **10**, 227 (1999).
[6]S. Nakamura, M. Senoh, S.-I. Nagahama, N. Iwasa, T. Yamada, T. Matsushita, H. Kiyoku, Y. Sugimoto, T. Kozaki, H. Umemoto, M. Sano, and K. Chocho, Appl. Phys. Lett. **72**, 211 (1998).
[7]F. A. Ponce and D. P. Bour, Nature Mater. **386**, 351 (1997).
[8]J. W. Orton and C. T. Foxon, Rep. Prog. Phys. **61**, 1 (1998).
[9]H. Morkoc, A. Di Carlo, and R. Cingolani, Solid-State Electron. **46**, 157 (2002).
[10]M. S. Shur, Solid-State Electron. **42**, 2131 (1998).
[11]S. Yoshida and H. Ishii, Phys. Status Solidi A **188**, 243 (2001).
[12]S. C. Binari, K. Doverspike, G. Kelner, H. B. Dietrich, and A. E. Wickenden, Solid-State Electron. **41**, 177 (1997).
[13]C.-C. Chen, C.-C. Yeh, C.-H. Chen, M.-Y. Yu, H.-L. Liu, J.-J. Wu, K.-H. Chen, L.-C. Chen, J.-Y. Peng, and Y.-F. Chen, J. Am. Chem. Soc. **123**, 2791 (2001).
[14]T. Kuykendall, P. J. Pauzauskie, S. Lee, Y. F. Zhang, J. Goldberger, and P. D. Yang, Nano Lett. **3**, 1063 (2003).
[15]K. A. Bertness, A. Roshko, L. M. Mansfield, T. E. Harvey, and N. A. Sanford, J. Cryst. Growth **300**, 94 (2007).
[16]W. Han, P. Redlich, F. Ernst, and M. Ruhle, Appl. Phys. Lett. **76**, 652 (2000).
[17]W.-Q. Han and A. Zettl, Appl. Phys. Lett. **80**, 303 (2002).
[18]D. K. T. Ng, L. S. Tan, and M. H. Hong, Curr. Appl. Phys. **6**, 403 (2006).
[19]B. Ha, S. H. Seo, J. H. Cho, C. S. Yoon, J. Yoo, G. C. Yi, C. Y. Park, and C. J. Lee, J. Phys. Chem. **109**, 11095 (2005).
[20]J. Yoo, Y.-J. Hong, S. J. An, G.-C. Yi, B. Chon, T. Joo, J.-W. Kim, and J.-S. Lee, Appl. Phys. Lett. **89**, 043124 (2006).
[21]C.-K. Sun, Y.-L. Huang, S. Keller, U. K. Mishra, and S. P. DenBaars, Phys. Rev. B **59**, 13535 (1999).
[22]O. Aoudé, P. Disseix, J. Leymarie, and A. Vasson, M. Leroux, E. Aujol, B. Beaumout, A. Trassoudaine, and Y. André, Phys. Rev. B **77**, 045206 (2008).
[23]E. D. O' Sullivan, S. Hess, R. A. Taylor, N. J. Cain, V. Roberts, J. S. Roberts, and J. F. Ryan, Physica B **272**, 402 (1999).
[24]B. Chon, S. R. Ryu, Y.-J. Hong, J. Yoo, G.-C. Yi, T. Joo, and Y. M. Jung, J. Mol. Struct. **883–884**, 209 (2008).
[25]J. Renard, B. Amstatt, C. Bougerol, E. Bellet-Amalric, B. Daudin, and B. Gayral, J. Appl. Phys. **104**, 103528 (2008).
[26]A. Othonos, J. Appl. Phys. **83**, 1789 (1998).
[27]X. M. Cai, A. B. Djurisic, and M. H. Xie, Thin Solid Films **515**, 984 (2006).
[28]J. Zhang and L. Zhang, J. Vac. Sci. Technol. B **21**, 2415 (2003).
[29]C. C. Tang, S. S. Fan, H. Y. Dang, P. Li, and Y. M. Liu, Appl. Phys. Lett. **77**, 1961 (2000).
[30]K.-W. Chang and J.-J. Wu, J. Phys. Chem. B **106**, 7796 (2002).
[31]L. Yu, Y. Ma, and Z. Hu, J. Cryst. Growth **310**, 5237 (2008).
[32]C.-K. Sun, J.-C. Liang, X.-Y. Yu, S. Keller, U. K. Mishra, and S. P. DenBaars, Appl. Phys. Lett. **78**, 2724 (2001).
[33]I. Shalish, L. Kronik, G. Segal, Y. Rosenwaks, Y. Shapira, U. Tisch, and J. Salzman, Phys. Rev. B **59**, 9748 (1999).
[34]Y. Xie, Y. Qian, and W. Wang, Science **272**, 1926 (1996).
[35]C. B. Soh, S. J. Chua, H. F. Lim, D. Z. Chi, S. Tripathy, and W. Liu, J. Appl. Phys. **96**, 1341 (2004).
[36]M. A. Reshchikov and H. Morkoc, J. Appl. Phys. **97**, 061301 (2005).